

See discussions, stats, and author profiles for this publication at: <https://www.researchgate.net/publication/253337199>

Unusual Through Space, TS, Pathway for the Transmission of (TS)JFH Coupling: 2-Fluorobenzaldehyde Study Case.

ARTICLE in THE JOURNAL OF PHYSICAL CHEMISTRY A · JULY 2013

Impact Factor: 2.69 · DOI: 10.1021/jp402618c · Source: PubMed

CITATIONS

2

READS

55

3 AUTHORS:



Denize Cristina Favaro

University of São Paulo

9 PUBLICATIONS 33 CITATIONS

SEE PROFILE



Rubén H Contreras

University of Buenos Aires

200 PUBLICATIONS 2,946 CITATIONS

SEE PROFILE



Claudio Tormena

University of Campinas

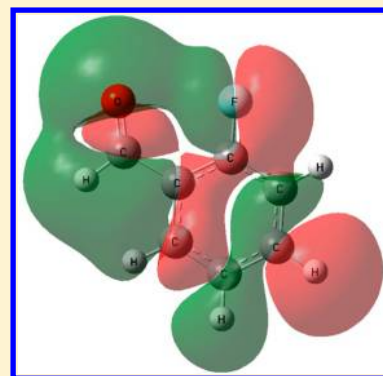
144 PUBLICATIONS 1,259 CITATIONS

SEE PROFILE

Unusual Through-Space, TS, Pathway for the Transmission of J_{FHf} Coupling: 2-Fluorobenzaldehyde Study CaseDenize C. Favaro,[†] Rubén H. Contreras,[‡] and Cláudio F. Tormena*,[†][†]Chemistry Institute, University of Campinas - UNICAMP, P.O. Box: 6154, 13084-862 Campinas, Sao Paulo, Brazil[‡]Department of Physics, FCEyN, University of Buenos Aires and IFIBA-CONICET, Buenos Aires, Argentina

S Supporting Information

ABSTRACT: The ^1H NMR spectra of the title compound in nonpolar and polar solvents and theoretical calculation of spin–spin coupling constants (SSCCs) show that $^{\text{TS}}J_{\text{FHf}}$ SSCC, where TS stands for “through-space”, in polar solvents is amenable to measurement only in the trans conformer. The mechanisms for transmission pathways to such unusual SSCCs are rationalized in terms of the molecular electronic structure. It is stressed that such a result calls for some caution when intending to use $^{\text{TS}}J_{\text{FH}}$ as a probe to detect the spatial proximity between fluorine and hydrogen atoms.



■ INTRODUCTION

Through-space spin–spin scalar coupling constants (TS-SSCCs) were reported for the first time in the early 1960s. The TS-SSCC pathway was reported to be due to interactions between proximate moieties^{1–7} and was assigned as responsible for the especially large SSCCs observed in many different systems, involving, among others, active nuclei such as ^1H , ^{13}C , ^{15}N , ^{19}F , and ^{31}P .^{8–18} Two of the most important TS-SSCCs are $^{\text{1h}}J_{\text{15N–1H}}$ and $^{\text{2h}}J_{\text{15N–15N}}$ couplings observed for DNA and RNA molecular systems,^{19,20} where the transmission pathway occurs through a hydrogen bond between Watson–Crick base pairs.²¹ Unusual through-space (TS) $^{\text{TS}}J_{\text{HH}}$ couplings have been observed across two stacked aromatic rings.^{22,23}

Due to the importance of the fluorine atom in medicinal chemistry,²⁴ interest in ^{19}F NMR is gaining attention^{25,26} due to its application as a tool to investigate new active molecules²⁷ to evaluate the quality of pharmaceutical formulations²⁸ to mark nucleosides and nucleotides to study their folding and binding sites and so forth. Although ^{19}F NMR applications are increasing, several aspects involving the transmission mechanism of the through-bond²⁹ and TS^{30,31} coupling constant ($^{\text{TS}}J$) are not always clear, and some effort to rationalizing such cases is a worthy aim.

Recently, it was shown³⁰ that in 2-fluorophenols, $^{\text{TS}}J_{\text{FH}}$ couplings are not transmitted through a hydrogen bond, as previously accepted.³² Instead, such $^{\text{TS}}J_{\text{FH}}$ couplings were shown to be mainly transmitted by exchange interactions taking place in the region where F and OH electronic clouds overlap. A critical evaluation study³¹ supports the hypothesis that the TS transmission of $^{\text{TS}}J_{\text{FH}}$ SSCCs are built up from different types of contributions, namely, (a) those originating in exchange interactions taking place in the region where

electronic clouds surrounding the F and H atoms overlap, (b) direct charge-transfer interactions between either $\text{LP}_{1,2,3}(\text{F})$ or $\sigma_{\text{C–F}}$ occupied and $\sigma_{\text{C–H}}^*$ vacant orbitals, and (c) long-range charge-transfer interactions mediated by concatenated sequences of hyperconjugative interactions. Type (a) contributions are positive for $\sigma_{\text{C–F}}/\sigma_{\text{C–H}}$ overlapping orbitals, while they are negative when they correspond to $\text{LP}_{1,2,3}(\text{F})/\sigma_{\text{C–H}}$ overlapping orbitals.³¹ However, the latter are operating only if for $\text{LP}_2(\text{F})$ and/or $\text{LP}_3(\text{F})$, the respective s % character is different from zero. On the other hand, contributions of types (b) and (c) correspond to positive contributions to the FC term of $^{\text{TS}}J_{\text{FH}}$. It was also observed³³ that steric interactions on a fluorine atom bonded to an aromatic system can affect the s % character of the $\text{LP}_2(\text{F})$ nonbonding electron pair.

To broaden the understanding of $^{\text{TS}}J_{\text{FH}}$ TS coupling constant transmission mechanisms, experimental and theoretical studies for 2-fluorobenzaldehyde (Figure 1) were performed, and unusual transmission pathways for $^{\text{TS}}J_{\text{FH}}$ are discussed in detail.

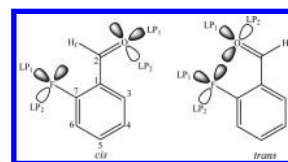


Figure 1. 2-Fluorobenzaldehyde and its two possible orientations for the formyl group. Representations for the LP_1 and LP_2 for oxygen and fluorine atoms are shown.

Received: March 15, 2013

Revised: July 29, 2013

Published: July 29, 2013

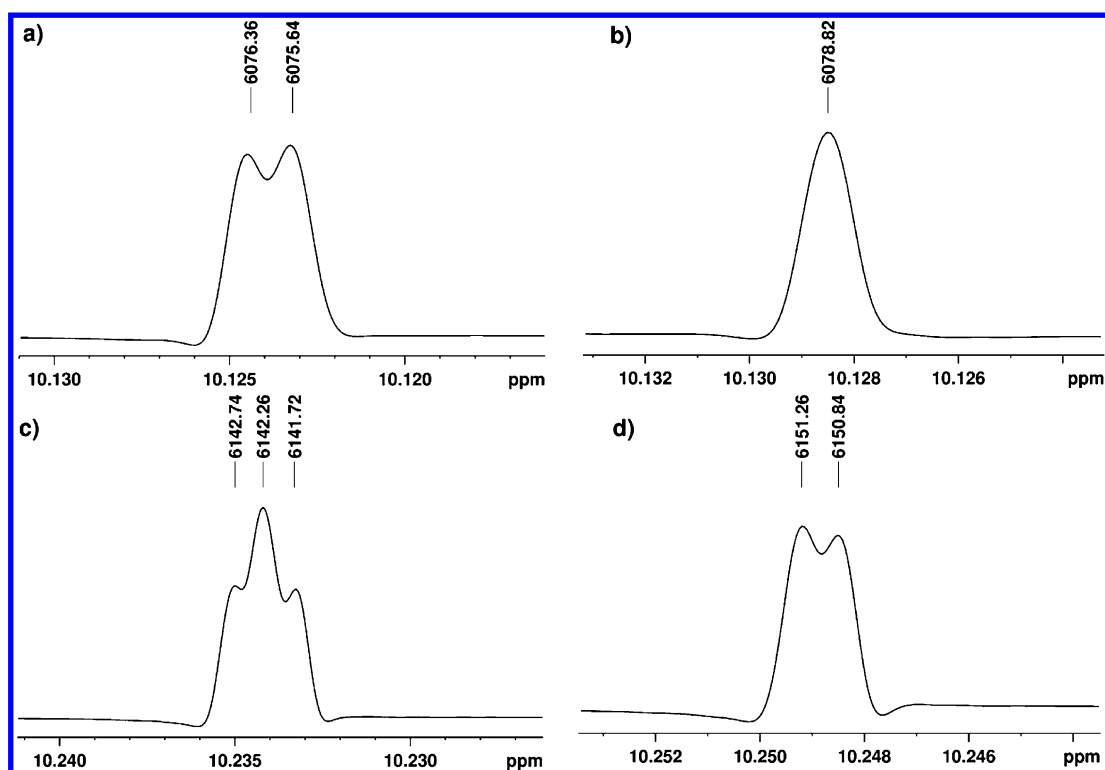


Figure 2. Formyl proton signals from ^1H NMR spectra for 2-fluorobenzaldehyde (a) in benzene- d_6 , (b) aromatic protons homodecoupled (in benzene- d_6), (c) in DMSO- d_6 , and (d) aromatic protons homodecoupled (in DMSO- d_6).

EXPERIMENTAL AND COMPUTATIONAL DETAILS

(a). NMR Measurements. The $^{\text{TS}}J_{\text{FH}}$ coupling constant for 2-fluorobenzaldehyde was measured from ^1H NMR spectrum, and unequivocal assignment was obtained from ^1H – ^1H COSY and ^1H – ^{19}F long-range correlation experiments using a Bruker standard hfcqfqn pulse sequence; long-range coupling (cnst11) was adjusted for 2 Hz. These experiments were performed on a Bruker Avance III 500 spectrometer equipped with a BBFO 5 mm smart probe with the z-gradient operating at 499.87 and 470.29 MHz for ^1H and ^{19}F , respectively. Samples were prepared as solutions of 10 mg of solute in 0.7 mL for solvents benzene- d_6 and DMSO- d_6 .

(b). Computational Details. Geometry optimizations and energy calculations for cis and trans conformers of 2-fluorobenzaldehyde were carried out at the MP2 level by applying two different basis sets, namely, aug-cc-pVTZ³⁴ and EPR-III,³⁵ using the Gaussian09 suite of programs³⁶ to perform them. $^{\text{TS}}J_{\text{FH}}$ SSCCs (as mentioned above, TS stands for through-space) were calculated at the SOPPA(CCSD)^{37–39} level using optimized geometries through the Dalton 2.0 program⁴⁰ employing the EPR-III³⁵ basis set. To study the solvent effect defining the preferential conformation for 2-fluorobenzaldehyde, geometry optimizations were performed, applying the SMD model⁴¹ at the MP2/aug-cc-pVTZ level. The Cartesian coordinates are supplied in the Supporting Information. Hyperconjugative interactions were evaluated using the natural bond orbital (NBO 5.9)⁴² analysis, as implemented in Gaussian 09, using the B3LYP^{43–45} hybrid functional employing the cc-pVTZ basis set.

RESULTS AND DISCUSSION

From the ^1H NMR spectrum for 2-fluorobenzaldehyde in nonpolar solvent (benzene- d_6), a doublet for the formyl proton

Table 1. Energies for 2-Fluorobenzaldehyde cis and trans Conformers and Molar Fraction for the Former Calculated at the MP2/aug-cc-pVTZ Theoretical Level

solvent	E_{cis}^a	E_{trans}^a	ΔE^b	n_{cis}
isolated molecule	−444.031731	−444.028321	2.1	0.97
benzene	−444.041117	−444.038621	1.6	0.94
DMSO	−444.040899	−444.039893	0.6	0.73

^aAtomic unit. ^bUnits: kcal mol^{−1}.

Table 2. J_{FHf} SSCCs Calculated at the SOPPA(CCSD)/EPR-III//MP2/EPR-III Level for cis and trans Conformers of 2-Fluorobenzaldehyde

conformation	cis	trans
$^{\text{FC}}J_{\text{FHf}}$	0.05	−1.84
$^{\text{SD}}J_{\text{FHf}}$	−0.17	−0.31
$^{\text{PSO}}J_{\text{FHf}}$	−0.75	0.99
$^{\text{DSO}}J_{\text{FHf}}$	1.41	−1.42
$^{\text{total}}J_{\text{FHf}}$	0.55	−2.58

(H_f) (Figure 2a) is observed, while in polar solvent (DMSO- d_6), this signal is observed as a triplet (Figure 2c). At first sight, this suggests that the formyl proton is coupled to only one aromatic proton in nonpolar solvents and two of them in polar solvents. However, when COSY contour plots for 2-fluorobenzaldehyde were obtained (Figures 1S and 2S, Supporting Information) in benzene- d_6 as well as in DMSO- d_6 solvents, only one correlation between the formyl proton (H_f) and aromatic protons was observed in both solvents, suggesting that in DMSO- d_6 , the formyl proton is coupled to the fluorine atom instead of two aromatic protons.

To verify this assertion, homodecoupled ^1H NMR experiments were performed for both samples (benzene- d_6 and

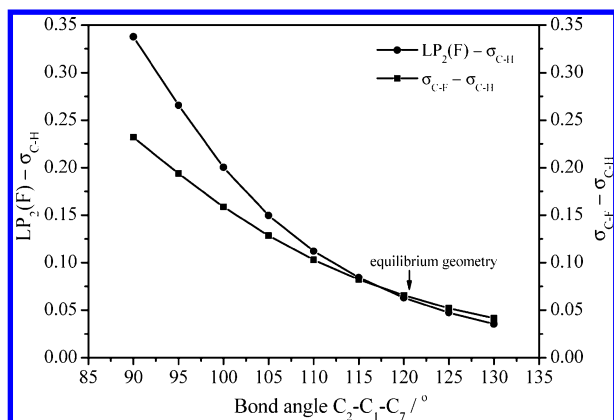


Figure 3. Variation of overlap between $LP_2(F)-\sigma_{C-Hf}$ and $\sigma_{C-F}-\sigma_{C-Hf}$ versus the bond angle for 2-fluorobenzaldehyde for the cis conformer.

DMSO- d_6), where aromatic protons were decoupled and the formyl proton was observed as a singlet for the benzene- d_6 sample (Figure 2b) and as a doublet for the DMSO- d_6 sample (Figure 2d).

To further confirm that the fluorine atom is coupled to the formyl proton, 2D $^{19}F-^1H$ NMR correlation experiments (HETCOR) were performed for 2-fluorobenzaldehyde using benzene- d_6 and DMSO- d_6 as solvents (Figures 3S and 4S, Supporting Information). As can be seen from contour plots in the Supporting Information for both samples, it is possible to observe a correlation between fluorine and formyl hydrogen.

Experimentally, it is unequivocal that there is a coupling constant between the H_f formyl proton and the fluorine nucleus ($J_{FH} = 0.48$ Hz, sign not determined) for 2-fluorobenzaldehyde when DMSO- d_6 is used as the solvent, while in benzene- d_6 , this coupling is too small to be measured but is not zero as was observed from HETCOR contour plot (Supporting Information). At this point, the main question that remains unanswered yet is, Why is this coupling constant observed when polar solvent is used?

As mentioned above, 2-fluorobenzaldehyde possesses two conformational arrangements for the formyl group (Figure 1); to determine which one is the most stable form in an isolated

molecule as well in solution, theoretical calculations at the MP2/aug-cc-pVTZ level are performed (Table 1).

According to results displayed in Table 1, the cis conformation is by far the more stable conformer when considering an isolated molecule. When the solvent effect is included in that calculation, the energy difference between cis and trans conformers reduces to $1.6 \text{ kcal mol}^{-1}$ in benzene and $0.6 \text{ kcal mol}^{-1}$ in DMSO. This difference in energy is expected because the calculated dipole moments for cis and trans conformers considering an isolated molecule are $\mu = 3.8$ and 5.2 D, respectively, explaining the larger stability for the trans conformer in polar solvent. This is good so far; however, the following question arises. In low polar media, the cis conformer is the most stable one, and although the fluorine atom and the formyl proton are closed in space, no $^{TS}J_{FH}$ SSCC is experimentally detected. In fact, the $^{TS}J_{FHf}$ SSCC is experimentally measured only when the sample is prepared in a polar solvent. According to results described above, in DMSO, the trans conformer population is around 26%. These results indicate that a $^{TS}J_{FH}$ coupling is only observed for the trans conformer, (Figure 1). In order to rationalize such a surprising experimental result, the J_{FHf} SSCCs were calculated for both conformers at the SOPPA(CCSD)/EPR-III//MP2/EPR-III level considering an isolated molecule. Results for the four Ramsey terms for J_{FHf} SSCCs thus obtained are displayed in Table 2.

The experimental $^{TS}J_{FHf}$ value measured in DMSO solution is 0.48 Hz, suggesting at first sight a good correlation with the cis conformation, but we need to keep in mind that the experimental value is an average between cis and trans conformations. When theoretical values listed at Table 2 were weighted using the population presented in Table 1 for DMSO solvent, the theoretical $^{TS}J_{FHf}$ coupling value in DMSO was -0.3 Hz, which is now in agreement with experimental (0.48 Hz) data.

It is interesting to rationalize, whenever possible, differences in the Ramsey contributions to both $^{TS}J_{FHf}$ couplings displayed in Table 2.

(a). About the FC Terms. Taking into account results reported recently³⁰ for *ortho*-fluorophenol, *cis*-FC = 0 Hz seems

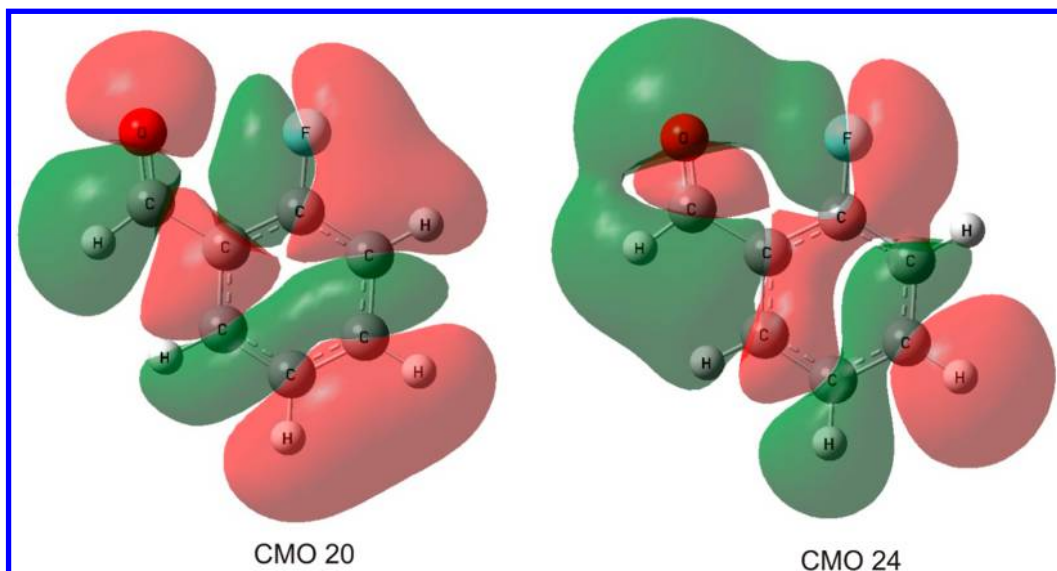


Figure 4. Plots of CMO 20 and CMO 24 for the 2-fluorobenzaldehyde trans conformer.

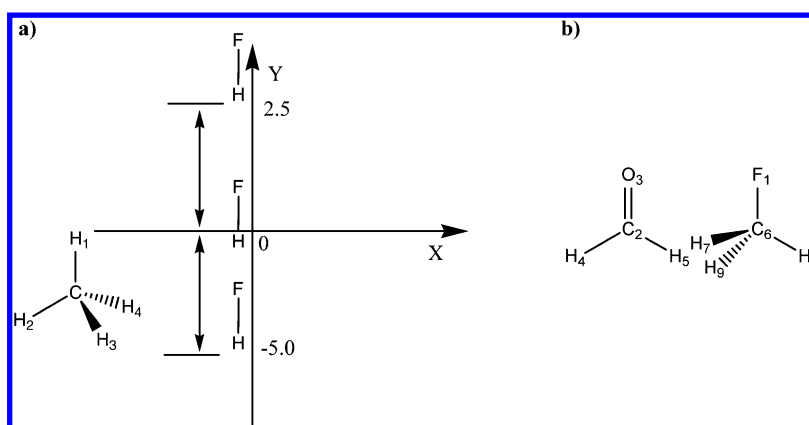


Figure 5. (a,b) Model systems are chosen to investigate different TS transmission mechanisms for the FC term for J_{FH} SSCCs like those described above for both conformers of 2-fluorobenzaldehyde. It is highlighted that in neither of the both model systems are there chemical bonds connecting the corresponding monomers.

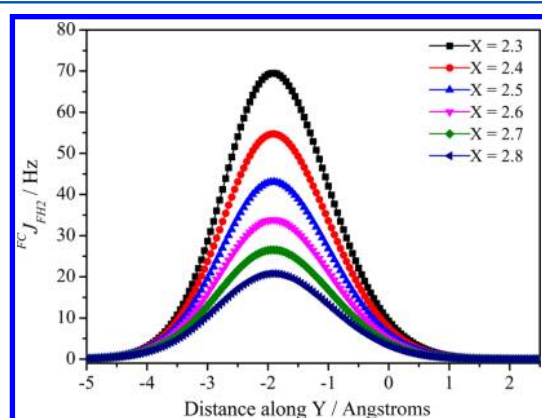


Figure 6. Variation of J_{FH2}^{FC} coupling for the methane...F–H model system for different arrangements for such a dimer.

to indicate that for the cis conformer, the $LP_{1,2,3}(F)/\sigma_{CH_F}$ and $\sigma_{C-F}/\sigma_{C-H_F}$ overlaps cancel each other. This conclusion is supported by calculating theoretically the overlaps between the corresponding *pre*-NBO overlaps, which show the same absolute values, and it is known⁴⁶ that such overlaps show opposite signs. See Figure 3.

For the trans conformer, the F...O distance is notably shorter than the sum of their van der Waals radii, 2.80 versus (1.47 + 1.52) Å = 2.99 Å, and therefore, there is a steric compression between the F and O atoms. In fact, NBO calculations show that the $LP_2(F)$ s % character is 0.32. Also, that steric interaction “contaminates” $LP_1(O)$ with the fluorine Fermi contact information. Therefore, an efficient coupling pathway is activated for transmitting the FC contribution to J_{FH} . According to theoretical calculations displayed in Table 2, this FC term is negative. It is recalled that the sign of this coupling could not be determined experimentally.

(b). About the SD Terms. Their cis and trans conformers show the smallest difference for the four terms; therefore, it is not worth performing a qualitative analysis of such a small difference.

(c). About the PSO Terms. The rationalization for the PSO difference for cis and trans conformers is straightforwardly obtained by employing the qualitative analysis discussed in previous papers.^{29–31} Within this qualitative approach, each PSO term tensor component can be written in terms of NBO contributions as in eq 1, where α is a Cartesian coordinate. The i and j stand for occupied NBOs, and a and b stand for vacant NBOs.

$$J_{ia,jb}^{TS, PSO\alpha\alpha}(F, H) = U_{ia,F}^{PSO,\alpha} W_{ia,jb} U_{jb,H}^{PSO,\alpha} \quad (1)$$

where

$$U_{ia,F}^{PSO,\alpha} = \langle i | \frac{(\vec{r}_F \times \vec{\nabla})_\alpha}{r_F^3} | a \rangle \quad \text{and} \quad U_{jb,H}^{PSO,\alpha} = \langle j | \frac{(\vec{r}_H \times \vec{\nabla})_\alpha}{r_H^3} | b \rangle \quad (2)$$

are the “perturbators”, which show vector character (actually, pseudo vector); they constitute the “emission/receptor” system corresponding to those NBOs. The transmission system is given by the $W_{ia,jb}$ matrix. The PSO tensor character originates in the tensor product between both perturbators, eq 2. The physical meaning for each perturbator is quite easy to visualize. For instance, that centered at the F atom corresponds to the overlap between the 90° rotated i occupied NBO and the a vacant NBO, divided by the cubic distance to the F nucleus.

With this brief description, it is easy to rationalize the PSO difference for the cis and trans conformers displayed in Table 2.

Table 3. CMO Contributing to the FC Transmission for J_{FH} SSCC Expanded in Terms of NBOs for the Formaldehyde...Fluoromethane Model System

MO 8 (occ): $\epsilon = -0.633514$ au
0.615*[5]:BD(1)C2–H5
0.503*[4]:BD (1)C2–H4
–0.381*[7]:BD(1)C6–H8
–0.341*[16]:LP(1)O
0.229*[13]:LP(1)F

MO 9 (occ): $\epsilon = -0.534599$ au
–0.577*[4]: BD(1)C2–H4
–0.450*[7]: BD(1)C6–H8
0.292*[6]: BD(1)C6–H7
–0.264*[14]: LP(2)F
–0.236*[17]: LP(2)O

MO 12 (occ): $\epsilon = -0.444077$ au
–0.584*[16]: LP(1)O
–0.496*[4]: BD(1)C2–H 4
–0.343*[2]: BD (1)C2–O3
–0.313*[17]: LP(2)O
0.234*[14]: LP(2)F

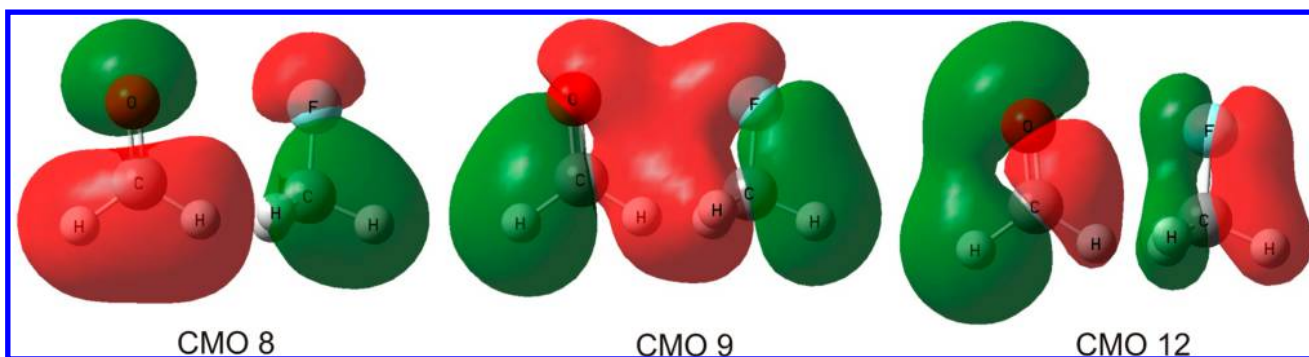


Figure 7. Plots of CMO 8, CMO 9, and CMO 12 for the formaldehyde...fluoromethane model.

For instance, for the *cis* conformation, when rotating $LP_2(F)$ around an axis perpendicular to the molecular plane, it overlaps with the formyl $(C-H)^*$ antibonding orbital, yielding a negative contribution to PSO.²⁹ For the *trans* conformer, such an overlap takes place between $LP_2(F)$ with the rear-lobe of the formyl $(C-H)^*$ antibonding orbital. The overlap matrix (S_{ij}) element was theoretically calculated for both conformations using NBO analysis,⁴² and for the *trans* conformer, this overlap was more efficient (-0.0564) than that for the *cis* (0.0159). When the sign of overlap between the occupied and vacant orbitals changes, the PSO contribution changes also its sign, as expected from our qualitative description.^{29,31}

(d). About the DSO Terms. The trend of the isotropic part of the DSO contribution to any SSCC follows a well-known trend.⁴⁷ In fact, if the space spanned by the electrons of the studied compound is divided into two different regions by a sphere whose diameter is just the $F\cdots H$ distance, then electrons within that sphere yield a positive contribution to the isotropic DSO term of J_{FH} SSCC. Those in the region outside of that sphere yield a negative contribution. Therefore, the DSO change in sign for *cis* and *trans* conformers is easily rationalized.

The rationalization presented above for the FC contribution to $^{TS}J_{FHF}$ SSCC is quite appealing, and it seems worth finding other results that could further support it. Such support can be found by resorting to a method recently reported and known by its acronym FCCP-CMO,⁴⁸ which stands for “Fermi contact coupling pathways detected using canonical molecular orbitals”. It is based on the known relationship between the Fermi hole and the FC interaction transmissions.⁴⁹ The main point is to determine the spatial region spanned by each CMO. This task is achieved by expanding each CMO in terms of NBOs, which can be accomplished using the NBO 5.9 program.⁴²

For the *trans* conformer, the FCCP-CMO analyses show that the $^{TS}J_{FHF}$ coupling transmission is mediated by virtual transitions between occupied and vacant CMOs, unless the FC interaction is mostly transmitted by exchange interactions, in which case, only occupied CMOs contain in their expansions in terms of NBOs both coupling nuclei. In the present case, only occupied CMOs contain simultaneously F and H_f nuclei, that is, CMOs 20 and 24 (Table 1S, Supporting Information). This indicates that the main transmission mechanism for the FC term for $^{TS}J_{FHF}$ SSCC is the exchange interaction in the region where the F and H_f electronic clouds overlap. CMOs 20 and 24 in their NBO expansions both contain $LP_2(F)$ and $C-H_f$ bonding orbitals. Plots for such CMOs for the 2-fluorobenzaldehyde *trans* conformer are displayed in Figure 4. It is recalled that a steric compression on $LP_2(F)$ increases its s % character. In this particular case, it increases from 0.00 to

0.32%. It is known⁵⁰ that only MOs with a significant s character on both coupled nuclei contribute to its FC contribution. For the *cis* conformation, the $F\cdots H_f$ proximity does not produce a strong steric interaction like that mentioned above for the *trans* conformer, and consequently, its $LP_2(F)$ s % character is about 15 times smaller (0.02%) than that for the *trans* conformer. Besides, for this conformation, there is a competition between the $C-H_f/F-C_2$ and $C-H_f/LP_1(F)$ overlaps where exchange interactions take place and lead to opposite sign contributions to the FC term (see Figure 3)³¹ and only a very small contribution to $^{TS}J_{FHF}$ remains, in agreement with the experimental observations described above. It is highlighted that plots displayed in Figure 4 nicely support that FC rationalization. This description leads to an adequate rationalization for the FC contribution to $^{TS}J_{FHF}$ in both *cis* and *trans* conformers for 2-fluorobenzaldehyde.

In order to reinforce our rationalization about the TS and through-bond transmission mechanisms for $^{TS}J_{FHF}$ SSCCs, two very simple models (Figure 5) are chosen where there are no chemical bond sequences connecting both coupling nuclei. In this way, it is obvious that intermolecular couplings are transmitted through space.

For the first model system (Figure 5a), geometries for methane and H–F molecules were optimized separately, and its dimer was built up by taking the H–F bond parallel to the $C-H_1$ methane bond, defining a methane bisector plane. To mimic the J_{FHF} TS coupling in *trans*-2-fluorobenzaldehyde, calculations for J_{FH2} SSCC were performed for that configuration, running X from 2.3 to 2.8 Å and, for each point, running Y from -5 to $+2$ Å, in 0.1 Å steps. In this way, the six plots shown in Figure 6 were obtained. All of these SSCC calculations were performed at the BHandH/EPR-III level.

In Figure 6, the plot for $X = 2.3$ Å, $^{FC}J_{FH2}$ coupling increases up to 70 Hz for $Y = -1.9$ Å and then decreases to 0 Hz for $Y = -5.0$ Å. It is stressed that SSCC values shown in Figure 6 are transmitted through space between F and H_2 atoms because they are not connected by a sequence of chemical bonds. An important contribution to this FC interaction is transmitted by the $LP_2(F) \rightarrow \sigma^*_{C1-H2}$ hyperconjugative interaction, which strongly depends on the overlap between the $C-H_2$ bond and the $LP_2(F)$ lone pair. However, it is not the most adequate model to mimic the FC term for $^{TS}J_{FHF}$ in *trans*-2-fluorobenzaldehyde because the latter is negative while those displayed in Figure 6 are positive. Therefore, to get a closer model system for 2-fluorobenzaldehyde, the formaldehyde...fluoromethane dimer (Figure 5b) is now chosen.

The model shown in Figure 5b is built up by keeping the carbonyl group and the C–F bond in the same configuration as

those in the trans conformer of 2-fluorobenzaldehyde, and the remaining atoms are replaced to get the formaldehyde...fluoromethane model system (atomic coordinates for this system can be found in the Supporting Information). The J_{FHF} SSCC for this model was calculated at the SOPPA(CCSD)/EPR-III level, obtaining $^{\text{FC}}J_{\text{F1H4}} = -33.9$ Hz, a result that corroborates our conclusion that J_{FHF} SSCC in 2-fluorobenzaldehyde is transmitted through space instead of through bond because in this model (Figure 5b), there are no chemical bonds connecting the coupled nuclei. Besides, its sign is opposite to that calculated for a similar SSCC in the model displayed in Figure 5a.

The FCCP-CMO analysis for the FC term of the J_{FHF} SSCC calculated for the model system shown in Figure 5b is now discussed. The main contributions to that FC term originate in the canonical molecular orbitals (Table 3) CMO 8, CMO 9, and CMO 12, which are plotted in Figure 7. These are the main contributions to the FC term for the J_{FHF} SSCC, and they resemble those displayed in Figure 4 for *trans*-2-fluorobenzaldehyde.

CONCLUSION

Results discussed above call for some caution when intending to use $^{\text{TS}}J_{\text{FHF}}$ for determining the formyl preferential conformation in aromatic compounds containing a F atom adjacent to an aldehyde group. It is also highlighted that results discussed in this work support observations reported previously about transmission mechanisms for transmitting through space the FC interaction for J_{FH} SSCCs.

It is highlighted that results discussed above for the cis conformer show that the FC contribution to the $^{\text{TS}}J_{\text{FHF}}$ SSCC is close to zero when the calculated LP(F)/C–H_f and C–F/C–H_f overlaps almost cancel each other. It is also important to highlight the different signs for the PSO isotropic contribution to $^{\text{TS}}J_{\text{FH}}$ SSCCs for cis and trans conformers. This supports nicely the qualitative description shown above, which predicts opposite signs for such contributions.

ASSOCIATED CONTENT

Supporting Information

Full citation for ref 36, 2D NMR contour plots for 2-fluorobenzaldehyde, expansion of CMOs, and atomic coordinates and energies for the different conformers. This material is available free of charge via the Internet at <http://pubs.acs.org>.

AUTHOR INFORMATION

Corresponding Author

*E-mail: tormena@iqm.unicamp.br.

Notes

The authors declare no competing financial interest.

ACKNOWLEDGMENTS

C.F.T. is grateful to FAPESP for financial support (2011/17357-3) of this work and to CNPq for a fellowship (C.F.T.) and a scholarship to D.C.F. R.H.C. gratefully acknowledges economic support from CONICET (PIP 0369) and UBACYT, Programación Científica 2011–2014.

REFERENCES

(1) Petrakis, L.; Sederholm, C. H. NMR Fluorine–Fluorine Coupling Constants in Saturated Organic Compounds. *J. Chem. Phys.* **1961**, *35*, 1243–1248.

(2) Ng, S.; Sederholm, C. H. Nuclear Magnetic Resonance Fluorine–Fluorine Coupling Constants. *J. Chem. Phys.* **1964**, *40*, 2090–2094.

(3) Mallory, F. B.; Mallory, C. W.; Fedarko, M. C. Substituent Effects on Through-Space Fluorine–Fluorine Coupling in the 1,8-Difluoronaphthalene System. *J. Am. Chem. Soc.* **1974**, *96*, 3536–3542.

(4) Barfield, M.; Karplus, M. Valence-Bond Bond-Order Formulation for Contact Nuclear Spin–Spin Coupling. *J. Am. Chem. Soc.* **1969**, *91*, 1–10.

(5) Hirao, K.; Nakatsuji, H.; Kato, H.; Yonezawa, T. Theoretical Study of the Fluorine–Fluorine Nuclear Spin Coupling Constants. I. Importance of Orbital and Spin Dipolar Terms. *J. Am. Chem. Soc.* **1972**, *94*, 4078–4087.

(6) Hirao, K.; Nakatsuji, H.; Kato, H.; Yonezawa, T. Theoretical Study of the Fluorine–Fluorine Nuclear Spin Coupling Constants. II. Stereochemical Dependences. *J. Am. Chem. Soc.* **1973**, *95*, 31–41.

(7) Mallory, F. B. Theory Regarding the Role of Lone-Pair Interactions in Through-Space Fluorine–Fluorine Nuclear Spin–Spin Coupling. *J. Am. Chem. Soc.* **1973**, *95*, 7747–7752.

(8) Mallory, F. B.; Mallory, C. W.; Ricker, W. M. Nuclear Spin–Spin Coupling via Nonbonded Interactions. III. Effects of Molecular Structure on Through-Space Fluorine–Fluorine and Hydrogen–Fluorine Coupling. *J. Am. Chem. Soc.* **1975**, *97*, 4770–4771.

(9) Mallory, F. B.; Mallory, C. W.; Ricker, W. M. Nuclear Spin–Spin Coupling via Nonbonded Interactions. 4. Fluorine–Fluorine and Hydrogen–Fluorine Coupling in Substituted Benzo[c]phenanthrenes. *J. Org. Chem.* **1985**, *50*, 457–461.

(10) Mallory, F. B.; Luzik, E. D.; Mallory, C. W.; Carroll, P. J. Nuclear Spin–Spin Coupling via Nonbonded Interactions. 7. Effects of Molecular Structure on Nitrogen–Fluorine Coupling. *J. Org. Chem.* **1992**, *57*, 366–370.

(11) Krccmar, L.; Grunenberg, J.; Dix, I.; Jones, P. G.; Ibrom, K.; Ernst, L. Spin–Spin Interactions Across the “Cove” in the (Z) and (E) Isomers of 1,1'-Difluoro-9,9'-bifluorenylidene. *Eur. J. Org. Chem.* **2005**, 5306–5312.

(12) Hierso, J.-C.; Fihri, A.; Ivanov, V. V.; Hanquet, B.; Pirio, N.; Donnadiu, B.; Rebiere, B.; Amardeil, R.; Meunier, P. “Through-Space” Nuclear Spin–Spin J_{pp} Coupling in Tetrakisphosphine Ferrocenyl Derivatives: A ^{31}P NMR and X-ray Structure Correlation Study for Coordination Complexes. *J. Am. Chem. Soc.* **2004**, *126*, 11077–11087.

(13) Hierso, J.-C.; Evrad, D.; Lucas, D.; Richard, P.; Cattey, H.; Hanquet, B.; Meunier, P. “Through-Space” ^{31}P Spin–Spin Couplings in Ferrocenyl Tetrakisphosphine Coordination Complexes: Improvement in the Determination of the Distance Dependence of J_{pp} Constants. *J. Organomet. Chem.* **2008**, *693*, 574–578.

(14) Thomas, D. A.; Ivanov, V. V.; Butler, I. R.; Horton, P. N.; Meunier, P.; Hierso, J.-C. Coordination Chemistry of Tetra- and Tridentate Ferrocenyl Polyphosphines: An Unprecedented [1,1'-Heteroannular and 2,3-Homoannular]-Phosphorus-Bonding Framework in a Metallocene Dinuclear Coordination Complex. *Inorg. Chem.* **2008**, *47*, 1607–1615.

(15) Loening, N. M.; Anderson, C. E.; Iskenderian, W. S.; Anderson, C. D.; Rychnovsky, S. D.; Barfield, M.; O'Leary, D. J. Qualitative and Quantitative Measurements of Hydrogen Bond Mediated Scalar Couplings in Acyclic 1,3-Diols. *Org. Lett.* **2006**, *8*, 5321–5323.

(16) Takemura, H.; Ueda, R.; Iwanaga, T. C–F...HO Hydrogen Bond in 8-Fluoro-4-methyl-1-Naphthol. *J. Fluor. Chem.* **2009**, *130*, 684–688.

(17) Takemura, H.; Kaneko, M.; Sako, K.; Iwanaga, T. The Intramolecular C–F...HO Hydrogen Bond of 2-Fluorophenylidiphenylmethanol. *New J. Chem.* **2009**, *33*, 2004–2006.

(18) Kreutz, C.; Micura, R. *Modified Nucleosides in Biochemistry, Biotechnology and Medicine*; Herdewijn, P., Ed.; Wiley-VCH: Verlag GmbH & Co, KGaA: Weinheim, Germany, 2008; Chapter 1, p 3.

(19) Dingley, J.; Grzesiek, S. Direct Observation of Hydrogen Bonds in Nucleic Acid Base Pairs by Internucleotide $^2J_{\text{NN}}$ Couplings. *J. Am. Chem. Soc.* **1998**, *120*, 8293–8297.

(20) Pervushin, K.; Ono, A.; Fernandez, C.; Szyperki, T.; Kainosho, M.; Wüthrich, K. NMR Scalar Couplings across Watson–Crick Base Pair Hydrogen Bonds in DNA Observed by Transverse Relaxation-

Optimized Spectroscopy. *Proc. Natl. Acad. Sci. U.S.A.* **1998**, *95*, 14147–14151.

(21) Cybulski, H.; Sadlej, J. A Computational Study of the Nuclear Magnetic Resonance Parameters for Double Proton Exchange Pathways in the Formamide–Formic Acid and Formamide–Formamidine Complexes. *Phys. Chem. Chem. Phys.* **2009**, *11*, 11232–11242.

(22) Bifulco, G.; Mangoni, A. ^1H – ^1H Scalar Coupling Across Two Stacked Aromatic Rings: DFT Calculations and Experimental Proof. *Magn. Reson. Chem.* **2008**, *46*, 199–201.

(23) Dračinský, M.; Jansa, P.; Bour, P. Computational and Experimental Evidence of Through-Space NMR Spectroscopic J Coupling of Hydrogen Atoms. *Chem.—Eur. J.* **2012**, *18*, 981–986.

(24) Purser, S.; Moore, P. R.; Swallowb, S.; Gouverneur, V. Fluorine in Medicinal Chemistry. *Chem. Soc. Rev.* **2008**, *37*, 320–330.

(25) Kitevski-LeBlanc, J. L.; Prosser, R. S. Current Applications of ^{19}F NMR to Studies of Protein Structure and Dynamics. *Prog. NMR Spectrosc.* **2012**, *62*, 1–33.

(26) Qin, L.; Sheridan, C.; Gao, J. Synthesis of Tetrafluorinated Aromatic Amino Acids with Distinct Signatures in ^{19}F NMR. *Org. Lett.* **2012**, *14*, 528–531.

(27) Edmonds, M. K.; Graichen, F. H. M.; Gardiner, J.; Abell, A. D. Enantioselective Synthesis of α -Fluorinated β^2 -Amino Acids. *Org. Lett.* **2008**, *10*, 885–887.

(28) Trefi, S.; Gilard, V.; Balayssac, S.; Malet-Martino, M.; Martino, R. Quality Assessment of Fluoxetine and Fluvoxamine Pharmaceutical Formulations Purchased in Different Countries or via the Internet by ^{19}F and 2D DOSY ^1H NMR. *J. Pharm. Biomed. Anal.* **2008**, *46*, 707–722.

(29) Ducati, L. C.; Contreras, R. H.; Tormena, C. F. Unexpected Geometrical Effects on Paramagnetic Spin–Orbit and Spin–Dipolar $^2J_{\text{FF}}$ Couplings. *J. Phys. Chem. A* **2012**, *116*, 4930–4933.

(30) Cormanich, R. A.; Moreira, M. A.; Freitas, M. P.; Ramalho, T. C.; Anconi, C. P. A.; Rittner, R.; Contreras, R. H.; Tormena, C. F. ^1H J_{FH} Coupling in 2-Fluorophenol Revisited: Is Intramolecular Hydrogen Bond Responsible for This Long-Range Coupling? *Magn. Reson. Chem.* **2011**, *49*, 763–767.

(31) Contreras, R. H.; Ducati, L. C.; Tormena, C. F. Critical Analysis of the Through-Space Transmission of NMR J_{FH} Spin–Spin Coupling Constants. *Int. J. Quantum Chem.* **2012**, *112*, 3158–3163.

(32) Alkorta, I.; Elguero, J.; Denisov, G. S. A Review with Comprehensive Data on Experimental Indirect Scalar NMR Spin–Spin Coupling Constants across Hydrogen Bonds. *Magn. Reson. Chem.* **2008**, *46*, 599–624.

(33) Vilcachagua, J. D.; Ducati, L. C.; Rittner, R.; Contreras, R. H.; Tormena, C. F. Experimental, SOPPA(CCSD), and DFT Analysis of Substituent Effects on NMR $^1J_{\text{CF}}$ Coupling Constants in Fluorobenzene Derivatives. *J. Phys. Chem. A* **2011**, *115*, 1272–1279.

(34) Woon, D. E.; Dunning, T. H. Gaussian Basis Sets for Use in Correlated Molecular Calculations. III. The Atoms Aluminum through Argon. *J. Chem. Phys.* **1993**, *98*, 1358–1371.

(35) Barone, V. In *Recent Advances in Density Functional Methods, Part I*; Chong, D. P., Ed.; World Scientific Publishing Co.: Singapore, 1996.

(36) Frisch, M. J.; et al. *Gaussian 09*, revision B.01; Gaussian, Inc.: Wallingford, CT, 2010.

(37) Geertsens, J.; Oddershede, J. 2nd-Order Polarization Propagator Calculations of Indirect Nuclear Spin–Spin Coupling Tensors in the Water Molecule. *Chem. Phys.* **1984**, *90*, 301–311.

(38) Enevoldsen, T.; Oddershede, J.; Sauer, S. P. A. Correlated Calculations of Indirect Nuclear Spin–Spin Coupling Constants Using Second-Order Polarization Propagator Approximations: SOPPA and SOPPA(CCSD). *Theor. Chem. Acc.* **1998**, *100*, 275–284.

(39) Sauer, S. P. A. Second-Order Polarization Propagator Approximation with Coupled-Cluster Singles and Doubles Amplitudes-SOPPA(CCSD): The Polarizability and Hyperpolarizability of Li^- . *J. Phys. B: Atom. Mol. Opt. Phys.* **1997**, *30*, 3773–3780.

(40) Dalton2011, A Molecular Electronic Structure Program, Release 2011; see <http://daltonprogram.org> (2011).

(41) Marenich, A. V.; Cramer, C. J.; Truhlar, D. G. Universal Solvation Model Based on Solute Electron Density and on a Continuum Model of the Solvent Defined by the Bulk Dielectric Constant and Atomic Surface Tensions. *J. Phys. Chem. B* **2009**, *113*, 6378–6396.

(42) Glendening, E. D.; Badenhoop, J. K.; Reed, A. E.; Carpenter, J. E.; Bohmann, J. A.; Morales, C. M.; Weinhold, F. NBO 5.9; Theoretical Chemistry Institute, University of Wisconsin: Madison, WI, 2009; <http://www.chem.wisc.edu/~nbo5/>; Program as implemented in the Gaussian 09 package.

(43) Becke, A. D. Density-Functional Exchange-Energy Approximation with Correct Asymptotic Behavior. *Phys. Rev. A* **1988**, *38*, 3098–3100.

(44) Becke, A. D. Density-Functional Thermochemistry. III. The Role of Exact Exchange. *J. Chem. Phys.* **1993**, *98*, 5648–5652.

(45) Lee, T.; Yang, W. T.; Parr, R. G. Development of the Colle–Salvetti Correlation-Energy Formula into a Functional of the Electron Density. *Phys. Rev. B* **1988**, *37*, 785–789.

(46) Ruiz de Azúa, M. C.; Giribet, C. G.; Vizioli, C. V.; Contreras, R. H. Ab Initio IPPP-CLOPPA Approach to Perform Bond Contribution Analysis of NMR Coupling Constants: $^1J(\text{NH})$ in NH_3 as a Function of Pyramidalicity. *J. Mol. Struct.: THEOCHEM* **1998**, *433*, 141–150.

(47) Perez, J. E.; Ortiz, F. S.; Contreras, R. H.; Giribet, C. G.; Ruiz de Azúa, M. C. Analysis of the Diamagnetic Spin–Orbital Contribution to Indirect Nuclear Spin–Spin Coupling Constants. *J. Mol. Struct.: THEOCHEM* **1990**, *210*, 193–198.

(48) Contreras, R. H.; Gotelli, G.; Ducati, L. C.; Barbosa, T. M.; Tormena, C. F. Analysis of Canonical Molecular Orbitals to Identify Fermi Contact Coupling Pathways. I. Through-Space Transmission by Overlap of ^{31}P Lone Pairs. *J. Phys. Chem. A* **2010**, *114*, 1044–1051.

(49) Soncini, A.; Lazzeretti, P. Nuclear Spin–Spin Coupling Density Functions and the Fermi Hole. *J. Chem. Phys.* **2003**, *119*, 1343–1349.

(50) Autschbach, J.; Le Guennic, B. Analyzing and Interpreting NMR Spin–Spin Coupling Constants Using Molecular Orbital Calculations. *J. Chem. Educ.* **2007**, *84*, 156–171.